Theoretical Ecology manuscript No.
(will be inserted by the editor)

Synchronization in ecological systems by weak dispersal coupling with time delay

Emily Wall · Frederic Guichard · Antony R. Humphries

Received: date / Accepted: date

Abstract One of the most salient spatio-temporal patterns in population ecology is the synchronization of fluctuating local populations across vast spatial extent. Synchronization of abundance has been widely observed across a range of spatial scales in relation to rate of dispersal among discrete populations. However, the dependence of synchrony on patterns of among-patch movement across heterogeneous landscapes has been largely ignored. Here we consider the duration of movement between two predator-prey communities connected by weak dispersal, and its effect on population synchrony. More specifically, we introduce time delayed dispersal to incorporate the finite transmission time between discrete populations across a continuous landscape. Reducing the system to a phase model using weakly connected network theory, it is found that the time delay is an important factor determining the nature and stability of phase-locked states. Our analysis predicts enhanced convergence to stable synchronous fluctuations in general, and a decreased ability of systems to produce in-phase synchronization dynamics in the presence of delayed dispersal. These results introduce delayed dispersal as a tool for understanding the importance of dispersal time across a landscape matrix in affecting metacommunity dynamics. They further highlight the importance of landscape and dispersal patterns for predicting the onset of synchrony between weakly-coupled populations.

Keywords Synchronization · Phase model · Dispersal · Time delay

1 Introduction

Predicting the onset and maintenance of synchronous fluctuations of abundance among populations has led to important progress in the understanding of population persistence, species coexistence, and response to environmental change. However, most theoretical studies of synchrony have assumed instantaneous and passive movement of individuals among discrete habitats. In natural systems, discrete populations are typically embedded within a landscape matrix that constrains patterns and duration of movement between populations. It is thus important to predict the importance of such a landscape matrix on the emergence and stability of synchronous fluctuations of abundance between distant populations. Here we incorporate delayed dispersal as a means to study landscape and dispersal patterns between discrete predator-prey communities.

Synchronization is generally understood as a phenomenon where through interactions with one another, the timings of fluctuations in components of a dynamical system lock to a single pattern of variation in time. This concept arises in a variety of systems in physics, chemistry, social sciences, and biology: from crickets chirping in synchrony, to fireflies able to all flash in unison (Blasius and Tönjes 2007). Spatial

E. Wall · F. Guichard
Department of Biology, McGill University, Montreal, Canada
E-mail: emily.wall@mail.mcgill.ca

A.R. Humphries
Department of Mathematics and Statistics, McGill University, Montreal, Canada

synchronization in the context of population ecology refers to coincident changes in population characteristics such as abundance, reproduction, mortality, or mean size or age distribution, in geographically separated populations (Liebhold et al. 2004). Ecological examples of synchronization include the cycling of hare-lynx populations, where fluctuations of groups across Canada were found to be locked on the same tight ten-year cycle (Blasius and Tönjes 2007). Synchronized population dynamics have been observed in natural systems across a variety of taxa and spatial scales, from fungal plant pathogens across 0.5-3m, insect herbivores across 1-1000km, to birds across 5-2000km (Liebhold et al. 2004). For our purpose we study the synchrony of coupled oscillators, where individual populations undergo intrinsic oscillations in abundance with some natural frequency, and adjust their oscillations due to coupling (dispersal) between oscillators. This formalism has been used to predict the onset of synchrony in simple ecological systems (Goldwyn and Hastings 2008). Networks of time-delayed and weakly connected oscillators have also been studied in physics, engineering, and neurophysiology (Schuster and Wagner 1989, Dhamala et al. 2004, Campbell and Kobelevskiy 2012). However, no study has elucidated the role of delayed dispersal in coupled ecological systems.

Causes of spatial synchrony have been studied extensively across systems and scales. Coupled oscillator theory predicts that oscillators can be synchronized through direct coupling, or by external forcing. Equivalently in ecology, there are two main mechanisms that produce synchrony: (a) density-dependent direct interactions, namely dispersal between populations, and (b) what is known as the Moran effect (Moran 1953), which is the entrainment of systems with similar density-dependent dynamical structures by correlated density-independent external factors, such as climate or weather (Liebhold et al. 2004). Because most natural systems are connected through both dispersal and external stochastic fluctuations, and because both mechanisms produce similar patterns of synchrony it is often difficult to determine which factor or combination of factors underlies observed patterns of spatial synchrony.

Theory predicts that populations oscillating due to the same or slightly different density-dependent processes (linear or nonlinear) can be synchronized by dispersal of just a very small number of individuals per generation (Liebhold et al. 2004). However, if density-dependent processes are so different that populations oscillate with very different frequencies, then synchronization may not be possible through dispersal (Ranta et al. 1998). Besides dynamical stability of synchronization fluctuations, the rate of synchronization is another constraint on the ability of dispersal to explain synchrony in natural populations: dispersal-induced synchrony must converge rapidly to be observed (Goldwyn and Hastings 2008). Otherwise, populations will be kept in transient non-synchronous states by environmental perturbations. While strong coupling (i.e., a large number of species disperse per generation) can always increase convergence rates to synchrony in general, in a two predator-prey patch system connected only weakly by dispersal, the required property for fast convergence to synchrony is the separation on time scales between predator and prey dynamics (Goldwyn and Hastings 2008). This property is characteristic of relaxation oscillators where a large part of the cycle is spent at low population densities. In contrast, sinusoidal oscillators take a very long time to synchronize by weak dispersal. Our study examines some mechanisms underlying this result and uses its robustness to delayed dispersal to further predict characteristics of ecological systems that favour weak dispersal-induced synchronization.

Metapopulation theory and the study of fragmentation have emphasized discrete boundaries and movement between populations (Levins 1969, Hanski 1999). The appeal of metapopulation theory lies in its simplicity associated with the assumption of passive and instantaneous population movement between patches. As a result, model predictions applied to natural systems usually ignore the complex landscape matrix that provides the context for discrete populations (Brady et al. 2011, Turner et al. 2001): mountain peaks embedded in valleys, forest patches within meadows and seagrass and between coral reefs. Dispersing propagules and migrating individuals can spend significant time and show non random movement within such a landscape matrix depending on the nature of the movement and on distance between populations. Current metapopulation theory assumes that the spatial structure of metapopulations can be captured by a per capita dispersal rate alone, rather than dispersal time.

To better understand the mechanisms leading to synchronization in natural populations, we study the role of weak and delayed dispersal in driving the ecological conditions for the existence and stability of synchronous states, and for their resilience (convergence time). We illustrate how time delayed dispersal can be used to implement the particulars of individual movement (through active or passive dispersal) in the space between patches. While discrete patch models are useful for studying synchronization of spatially distributed systems from a dynamical systems point of view, they are associated with the assumption of instantaneous dispersal where individuals disperse with no transmission delay. By including

a time delay that retains more detailed information about the dispersal process, we extend the patch dynamics model to integrate properties of the landscape matrix that contains discrete populations. We next formulate an ecological model as a two-patch Rosenzweig-MacArthur predator prey model coupled through prey dispersal with a time delay. We reduce our model to a phase model using weakly-coupled network theory (Appendix A). Our results show that synchronization through weak dispersal is highly sensitive to dispersal time. We find that with slight variation in the delay, the overall influence of weak dispersal on the rate of convergence to synchrony can vary greatly. This means that dispersal time between spatially discrete systems is a key variable for assessing the role of weak dispersal as a cause of synchronous fluctuations in natural systems. We further extend recent results from Goldwyn and Hastings (2008) on synchronization between patches to predict the importance of such a matrix on the synchronization of weakly coupled predator-prey metacommunities.

2 Time-delay approach to modeling dispersal

Let us first articulate the relationship of patch dynamics with time delayed dispersal to other spatial dynamical frameworks. Durrett and Levin (1994) showed the importance of choosing an approach to modeling spatially distributed systems– mean field approaches, patch models, reaction-diffusion equations, or interacting particle systems– that captures the right level of spatial detail for understanding population dynamics. The time-delay model we will consider (see (3.2)) can be viewed as a combination of two existing treatments of spatial dynamics distinguished in this work. The system neglecting the time delay (i.e., for $s = 0$ in (3.2)) corresponds to the patch model approach: it groups individuals of a species into discrete patches without any spatially-explicit structure informing where patches are with respect to one another. In these models each patch is treated with a mean-field approach where individuals interact equally with each other and the patch itself is described by ordinary differential equations, and patches are connected to all others equally by dispersal or migration at a constant rate (Durrett and Levin 1994).

Patch models and mean-field approaches both lose the level of spatial detail required to account for the movement and local interactions of individuals both in the patch, and in dispersal between patches. The most common approach to modeling spatial systems working on a finer level of spatial detail are reaction-diffusion equations, in which infinitesimal individuals diffuse in space and undergo purely local interactions (reactions). The dispersal term in a patch model (say, $d(h_j(t)-h_i(t))$) can actually be derived from reaction-diffusion equations directly, through the discretization of continuous space, and we take a moment to illustrate this.

A common starting point for modeling random dispersal are diffusion equations, which are continuum approximations of discrete random walk processes. Individuals moving this way distribute over one-dimensional space and time according to the solution of the simple diffusion equation for an uncorrelated random walk:

$$\frac{\partial u}{\partial t} = D\frac{\partial^2 u}{\partial x^2}, \tag{2.1}$$

where D is a diffusion constant related to parameters like step size, the probability to make a turn at each step as opposed to not moving, and the time taken for a step or a pause. If we shift from continuous one-dimensional space to discrete space so that u_i is the density at point in space x_i, $i = 1, \ldots, n$, (2.1) becomes (for n=2):

$$\frac{du_i}{dt} = \frac{D}{l^2}\big[u_j(t) - u_i(t)\big], \quad i, j = 1, 2;\ i \neq j \tag{2.2}$$

where l is the distance between the patches. As shown by Allen (1983), this is the result of simply discretizing the second derivative in (2.1) and applying Neumann boundary conditions, which confine the individuals to the union of the two patches, allowing no movement in or out of them. Equation (2.2) is the patch model representation of dispersal: it distributes $u(x, t)$ over points in space representing the patches, so that information about the movement process between the patches is lost. It resembles the dispersal term in our main model (3.2), but without the incorporation of a time delay s for movement in the space between patches on the landscape matrix.

By treating space as continuous, our time-delay model avoids discretizing inter-patch space, keeping closer to the reaction-diffusion equation to describe dispersal in the space between patches. The addition of continuous space between patches (see Figure 1) as opposed to discretizing space allows for handling

the concept of diffusive dispersal closer to the more ecologically realistic formulation based on finite-speed random walks in the environment separating the patches, so that dispersers take some meaningful amount of time to cross from patch to patch. The model retains key features of actual movement as it makes a random walk between the patches through the value of the delay τ. Such features are lost in the discretized version with no delay. Furthermore, our time-delay dispersal is equivalent to the simplest case possible of the process of individuals reaction-diffusing in space: it assumes a constant mean dispersal duration, and no birth or mortality during dispersal. Under these assumptions we can equate incoming and outgoing population fluxes from the landscape matrix to the patches themselves, thereby incorporating the dispersal process into patch dynamics equations. The assumption of no birth or mortality during dispersal is not necessary for the analysis in Sections 3-5; however, it is crucial for our numerical computations (in particular for the computation of H using XPPAUT in Section 5).

In a system of patches connected by dispersal, the mean transmission time τ can be calculated in several ways using specific details of the individual dispersal process which might be easier to measure in natural systems than the time delay τ itself. We now demonstrate two such derivations. We start with a continuous space distribution of individuals dispersing in a one-dimensional connecting path between patches, according to some underlying assumptions about movement. We then uncover the net squared displacement of individuals in the path, which give the mean time an individual spends dispersing between two patches separated by a distance l.

If we first assume individuals move passively at a constant speed v with two-way travel on one-dimensional paths connecting patches, we can easily see that the mean crossing time τ in this case is just v/l. Suppose we consider the more general movement pattern integrating active dispersal modeled by the telegraph equation:

$$\frac{T}{2}\frac{\partial^2 u}{\partial t^2} + \frac{\partial u}{\partial t} = \frac{v^2 T}{2}\frac{\partial^2 u}{\partial x^2}, \tag{2.3}$$

where v is the finite speed of individual movement, and T is the characteristic time of movement before a direction reversal (see explanation in Turchin (1998) or derivation in Othmer and Dunbar (1988)). The mean squared displacement over time, $|x^2(t)|$, of a group of individuals instantaneously released into the system at patch 1 is calculated as follows in Othmer and Dunbar (1988):

$$|x^2(t)| = v^2 T\big[t - \frac{T}{2}(1 - e^{-2t/T})\big]. \tag{2.4}$$

While the mean displacement $|x(t)|$ is not quite equal to the square root of the mean squared displacement, one can scale $\sqrt{|x^2(t)|}$ by some factor C to obtain a better estimate for $|x(t)|$ than $\sqrt{|x^2(t)|}$ (Byers 2001). Then the mean displacement is then

$$|x(t)| = C\sqrt{v^2 T\big[t - \frac{T}{2}(1 - e^{-2t/T})\big]}. \tag{2.5}$$

Now set $|x(t)|$ in (2.5) to l and solve for the corresponding value of time t. This defines the delay s which appears in (3.2) as a function of l, T, and v. Note that the right hand side of (2.5) is a strictly monotonically increasing function of t, so there is a unique solution.

3 Ecological model

Following Goldwyn and Hastings (2008), we use the Rosenzweig-MacArthur predator-prey model for single-patch dynamics:

$$\begin{aligned} \frac{dH}{dt} &= rH\Big(1 - \frac{H}{K}\Big) - \frac{acPH}{b+H}, \\ \frac{dP}{dt} &= \frac{aPH}{b+H} - mP. \end{aligned} \tag{3.1}$$

Here $H(t)$ and $P(t)$ represent the size of the prey and predator populations respectively. Prey growth is modeled by logistic growth with intrinsic rate r and carrying capacity K, and the intake of prey by predators is modelled with a Holling Type II functional response specified by the parameters a and b and where the conversion ratio of loss of prey to increase in predators is $c > 1$. The predators have a linear mortality rate, with parameter m.

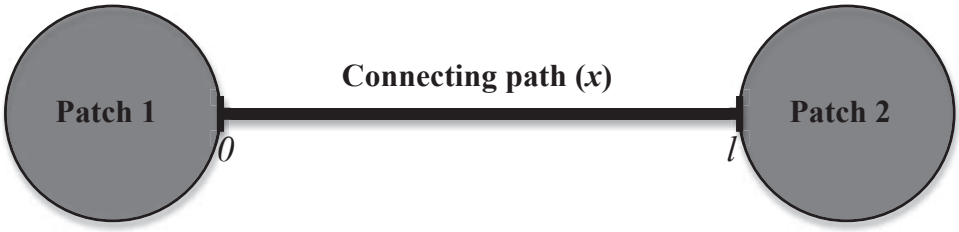

Fig. 1 Two discrete (homogeneous) patches connected by a one-dimensional (two-directional) path for dispersal.

Now suppose we have two identical and spatially discrete predator-prey patches, each with dynamics following (3.1). We consider the case where only prey disperse between patches with a fixed dispersing rate D. Naturally, the dispersing prey take some finite transmission time s to cross the space between the patches. When we further assume the absence of growth or mortality during dispersal, we can equate the incoming flux of individuals to a patch at time t with the outgoing flux of individuals at the opposite patch at a time $t - s$, before the present time. This allows us to incorporate the dispersal process into our four-equation model (where P_i and H_i represent the predator and prey populations in the ith patch) with just the term $D(H_j(t-s) - H_i(t))$ in the rate equation for the prey in the ith patch.

The result is the following two-patch Rosenzweig-MacArthur predator-prey model coupled through prey dispersal with a time delay:

$$\begin{aligned} \frac{dH_i}{dt} &= rH_i\Big(1 - \frac{H_i}{K}\Big) - \frac{acP_iH_i}{b + H_i} + D\big(H_j(t-s) - H_i(t)\big), \\ \frac{dP_i}{dt} &= \frac{aP_iH_i}{b + H_i} - mP_i, \qquad i, j = 1, 2; \;\; i \neq j. \end{aligned} \tag{3.2}$$

This is identical to the model studied by Goldwyn and Hastings (2008), except for the time delay of s time units that we include in the dispersal term, and that we allow only one of the species to disperse between patches.

We nondimensionalize (3.2) following Goldwyn and Hastings (2008) to reduce the number of parameters in a way that will be useful later for adjusting the timescale separation of the predator and prey growth rates. Thus we work with the following resulting equivalent form:

$$\begin{aligned} \frac{dh_i}{dt} &= \frac{1}{\varepsilon}\left(h_i(1 - \alpha h_i) - \frac{p_ih_i}{1 + h_i}\right) + d\big(h_j(t-\tau) - h_i(t)\big), \\ \frac{dp_i}{dt} &= \frac{p_ih_i}{1 + h_i} - \mu p_i, \qquad i, j = 1, 2; \;\; i \neq j, \end{aligned} \tag{3.3}$$

where we reuse the variable t for scaled time at, and make the following substitutions:
$h_i = H_i/b$, $p_i = [ac/rb]P_i$, $\tau = as$, $\alpha = b/K$, $\mu = m/a$, $\varepsilon = a/r$, $d = D/a$.

The single-patch dynamics of the Rosenzweig- MacArthur model are well-understood (Goldwyn and Hastings 2008). There is a region of ε–α–μ parameter space in which the dynamics produce a stable limit cycle, namely: $\alpha < 1$ and $\mu < \frac{1-\alpha}{1+\alpha}$. This is the case we are interested in for studying synchronization dynamics.

Furthermore, we are concerned with the part of ε–α–μ parameter space where the predator-prey oscillations are relaxation-like, since this leads to faster convergence to synchrony when the patches are weakly coupled, a requirement for weak dispersal to be the cause of synchronization in nature. Goldwyn and Hastings (2008) explains how the separation of timescales between the predator and prey leads the single-patch system to relaxation-like oscillations: in the nondimensionalized form (3.3), this is achieved by decreasing any one of ε, α, or μ. Decreasing ε increases the rate of intrinsic prey growth relative to that of the predator; decreasing α increases the carrying capacity for prey, enhancing the size and time between prey outbreaks; decreasing μ means slower predator mortality, which leads to longer times for the predator population to decrease to the point where the prey population spikes, so that these spikes happen less frequently (Goldwyn and Hastings 2008). In effect, the prey populations spend more time at low numbers and then grow more rapidly at spikes when ε, α, and μ are small.

4 Phase model

The purpose of this section is to reduce our ecological model to a phase model more practical to analyze. We use and refer to concepts of weakly connected network theory which are outlined in Appendix A.

Suppose we choose parameters ε, α, and μ for our model (3.3) so that the identical uncoupled subsystems (i.e., the two patches with $\delta = 0$) oscillate on an exponentially orbitally stable limit cycle $\gamma(t)$, which means that solutions starting close enough to the limit cycle approach it exponentially fast in the limit as time goes to infinity. The coupling in (3.3) is symmetric, so the system can be written in the general form for weakly connected networks as follows:

$$\begin{aligned}\dot{X}_1(t) &= F(X_1(t)) + \delta W(X_1(t), X_2(t-\tau))\\ \dot{X}_2(t) &= F(X_2(t)) + \delta W(X_2(t), X_1(t-\tau)),\end{aligned}$$

where

$$\begin{aligned}&X_i = (h_i, p_i)^T,\\ &F(X_i) = \left(\frac{1}{\varepsilon}\Big(h_i(1-\alpha h_i) - \frac{p_i h_i}{1+h_i}\Big), \frac{p_i h_i}{1+h_i} - \mu p_i\right)^T,\\ &W(X_i(t), X_j(t-\tau)) = (h_j(t-\tau) - h_i(t), 0)^T.\end{aligned} \tag{4.1}$$

Characterized by its shape, position and natural frequency Ω, each periodic solution γ is an isolated closed curve through two-dimensional phase space, a distorted circle that can be parameterized with a phase variable θ that increases by 2π in one period (see Appendix A).

When we consider the full system, the fact that the γ are exponentially orbitally stable limit cycle attractors means that for small δ, coupling between the X_i only significantly affects the phase variables θ_i. We assume that the time delay τ is of an order of magnitude of $2\pi/\Omega$ or less. Then, by the theorem in Appendix A we can reduce (4.1) to the corresponding two-dimensional phase model:

$$\begin{aligned}\frac{d\theta_1}{dt} &= \Omega + \delta H(\theta_2 - \theta_1 - \Phi)\\ \frac{d\theta_2}{dt} &= \Omega + \delta H(\theta_1 - \theta_2 - \Phi),\end{aligned} \tag{4.2}$$

where $\Phi = \Omega\tau \bmod 2\pi$ and

$$H(x) = \frac{1}{T}\int_0^T \hat{\gamma}(t) \cdot W(\gamma(t), \gamma(t + x/\Omega))\, dt, \tag{4.3}$$

with $\hat{\gamma}(t)$ solving the system

$$\begin{aligned}\frac{dz(t)}{dt} &= -DF(\gamma(t))^T z(t)\\ z(t) \cdot \gamma'(t) &= 1.\end{aligned} \tag{4.4}$$

Finally, we define the phase difference variable $\phi(t)$ as $\phi \equiv \theta_1 - \theta_2$. This reduces the system (4.2) further, to

$$\frac{d\phi}{dt} = G(\phi) := \delta[H(-\phi - \Omega\tau) - H(\phi - \Omega\tau)] \equiv \delta H_{delay}(\phi) \tag{4.5}$$

where we just denote Φ with $\Omega\tau$.

5 Phase model analysis

So far we have reduced the full system (4.1) to a one-dimensional dynamical system with variable ϕ that is directly related to synchrony: (4.5) relates the parameters ε, α, and μ using Ω and H, as well as a time delay τ, to the relative phase positions of the two oscillators in their limit cycle. Now suppose the dynamics $\phi(t)$ from any starting phase difference $\phi(t_0)$ converge with time to some fixed phase difference ϕ^* with $G(\phi^*) = 0$. We refer to this phenomenon as phase locking, and say that the system is in-phase synchronized when phase-locked at $\phi^* = 0$, and asynchronized when phase locked at $\phi^* \neq 0$.

We solve for H numerically using the numerical software XPPAUT (Ermentrout 2002). We first find the numerical solution of a single patch model with given parameters ε, α, and μ. We then calculate Ω, and the function $\hat{\gamma}(t)$ that solves (4.4) (the iPRC, discussed in Appendix A). XPPAUT can then can approximate the corresponding coupling function $H(x)$ (the calculation uses (4.3)). We obtain this function via its first eleven Fourier coefficients a_n and b_n, $n = 0, \ldots, 10$, which approximate

$$H(x) = \sum_{n=0}^{10} [a_n \cos(nx) + b_n \sin(nx)].$$

Now by a simple calculation (as done in Kobelevskiy (2008)), we define

$$\begin{aligned} H_{delay}(\phi) &= H(-\phi - \Omega\tau) - H(\phi - \Omega\tau) \\ &= -2 \sum_{n=0}^{10} \sin(n\phi)[a_n \sin(n\Omega\tau) + b_n \cos(n\Omega\tau)], \end{aligned}$$

so that calling $c_n = a_n \sin(n\Omega\tau) + b_n \cos(n\Omega\tau)$, we have an expression for $G(\phi) = \frac{d\phi}{dt}$:

$$G(\phi) = -2\delta \sum_{n=0}^{10} c_n \sin(n\phi). \tag{5.1}$$

Our approximation was not improved by using more than eleven Fourier coefficients. We can now integrate $G(\phi)$ in time to find the solution of the system for an arbitrary starting phase difference to investigate the effect of τ on phase dynamics.

6 Results

6.1 Phase-locked states

We begin by investigating the effects of a time delay for the parameter set $\varepsilon = 0.1$, $\alpha = 0.3$, and $\mu = 0.3$ in (3.3), which for an uncoupled patch (i.e., $\delta = 0$) leads to stable oscillatory dynamics with frequency $\Omega = 0.74199$. We use $\delta = 0.001$ for weak coupling. We retrieve our coefficients a_n and b_n to construct $G(\phi) = \frac{d\phi}{dt}$ from (5.1), which has roots corresponding to steady states. Notice that $G(\phi)$ is T-periodic in τ. Thus we examine a range of τ values from 0 to $T = 8.468 = 2\pi/\Omega$. This range is justified under the assumption that τ is of the same order of magnitude as T or less. If $G'(\phi^*) < 0$ at a steady-state ϕ^*, then it is stable, while if $G'(\phi^*) > 0$ then the steady state is unstable.

The number and stability of phase-locked solutions to the two-patch predator-prey system is strongly affected by delayed dispersal (Figure 3). We start with $\tau = 0$, equivalent to instantaneous travel between patches, and see that the system has two stable steady state solutions, 0 and π, and two unstable steady-state solutions at intermediate phase difference values (Figure 2 and 3). As τ is increased, 0 and π are always steady-state solutions because $G(\phi)$ is 2π periodic and odd. We see that other steady-state solutions may exist, appearing or disappearing in a total of ten saddle-node or pitchfork bifurcations as τ is varied from 0 to $T = 8.468$ (Figure 3).

Our bifurcation analysis reveals the complex response of phase dynamics to a time delay in dispersal. Super-critical pitchfork bifurcations occur at the steady state $\phi^* = 0$ when $\tau = 2.172$, and at the steady state $\phi^* = \pi$ when $\tau = 6.407$. In the bifurcation at $\tau = 2.172$, as can be seen in Figure 3(a), the steady state at $\phi^* = 0$ changes stability, and a branch of stable steady states bifurcates from $\phi^* = 0$ with the new stable branch existing for $\tau < 2.172$ where the $\phi^* = 0$ solution is unstable. There is thus a stable steady state at $\phi^* = 0$ on one side of the bifurcation, and a stable steady state close to 0 on the other side of the bifurcation. Thus at this bifurcation the $\phi^* = 0$ stable steady-state is carried continuously away from 0 (or the reverse). The behaviour at the other supercritical pitchfork bifurcation at $\phi^* = \pi$ when $\tau = 6.407$ is similar, except we see that there are actually two branches that bifurcate from $\phi^* = \pi$ in symmetric fashion. This is characteristic of all supercritical pitchfork bifurcations (and also occurs in the bifurcation at $\phi^* = 0$, $\tau = 2.172$ on noting that $\phi = 0$ and $\phi = 2\pi$ represent the same phase).

Sub-critical pitchfork bifurcations occur at $\phi^* = 0$ when $\tau = 0.0228$, 4.381 and 6.223 and at $\phi^* = \pi$ when $\tau = 0.1462$, 1.99 and 4.257. The bifurcations at $\phi^* = 0$ when $\tau = 4.381$ and 6.223 are clearly visible

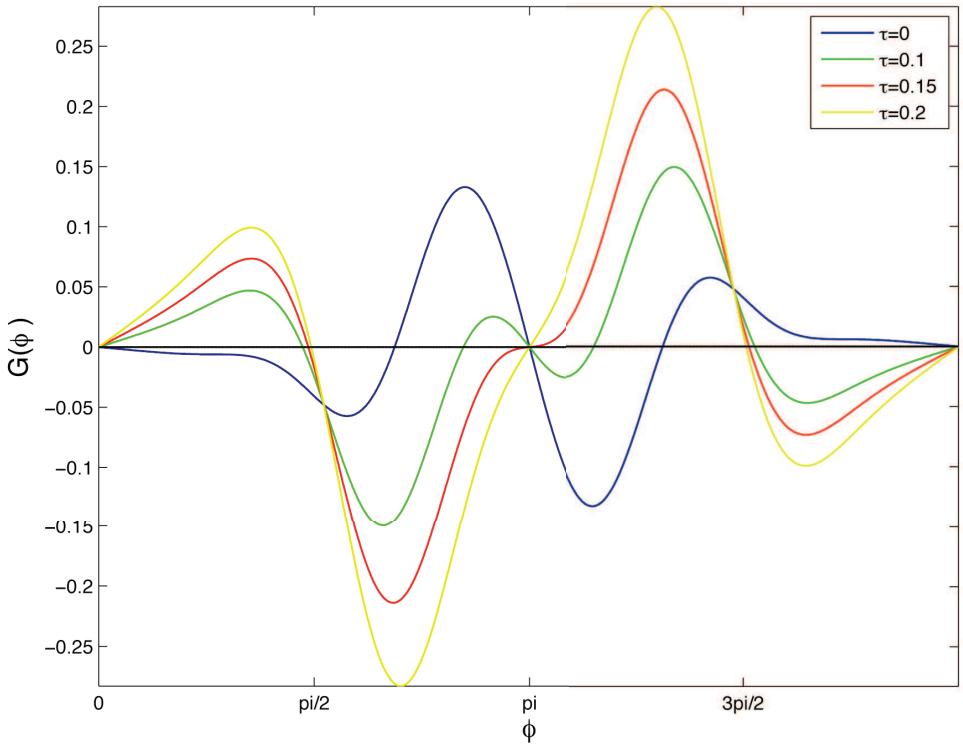

Fig. 2 $\varepsilon = 0.1$, $\alpha = 0.3$, $\mu = 0.3$, and $\delta = 0.001$. $G(\phi)$ for a few different values of τ.

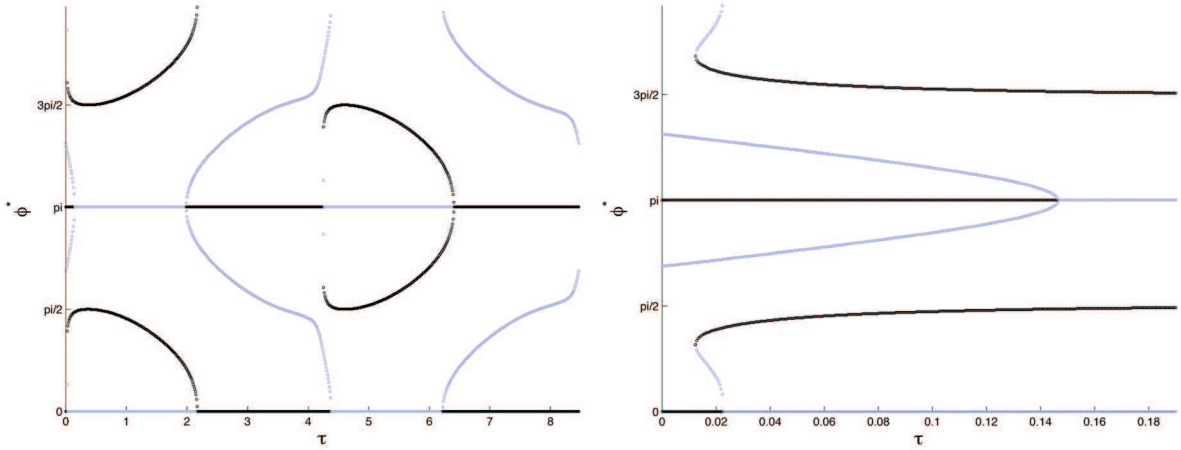

(a) (b)

Fig. 3 $\varepsilon = 0.1$, $\alpha = 0.3$, $\mu = 0.3$, and $\delta = 0.001$. τ-Bifurcation diagram: (a) showing a full τ range, (b) showing values for τ close to 0. Stable steady-states are black; unstable steady-states are blue (appearing as grey in monochrome).

in Figure 3(a), while the bifurcation at $\phi^* = 0$, $\tau = 0.0228$ can be seen in Figure 3(b). These are the most dynamically disruptive type of pitchfork bifurcation, since a stable steady state exists only on one side of these bifurcation points. A system in nature passing through such a bifurcation would 'jump' abruptly from one steady-state to another (outside the region of the bifurcation point).

Saddle-node bifurcations correspond to two steady states (one stable and one unstable) that collide and annihilate so that a stable steady state either appears or disappears. There are two such bifurcations in our system; the one at $\tau = 0.0124$ is clearly visible in Figure 3(b) occurring close to subcritical pitchfork bifurcation at $\tau = 0.0228$. The second saddle-node bifurcation occurs at $\tau = 4.247$, close to the subcritical pitchfork bifurcation at $\phi^* = \pi$ when $\tau = 4.257$. The separation of the τ values of these last two bifurcations is very small and they are difficult to distinguish in Figure 3(a), but the form of the bifurcation branches is similar to that of shown in Figure 3(b) for the other saddle-node bifurcation.

Table 1 $\varepsilon = 0.1$, $\alpha = 0.3$, $\mu = 0.3$, and $\delta = 0.001$. Stable steady states for varying τ values.

τ Range	Stable steady-states
(0, 0.0124)	0, π
(0.0124, 0.0228)	0, $0 < \phi^* < \pi$, π, -ϕ^*
(0.0228, 0.1462)	$0 < \phi^* < \pi$, π, -ϕ^*
(0.1462, 1.99)	$0 < \phi^* < \pi$, -ϕ^*
(1.99, 2.172)	$0 < \phi^* < \pi$, π, -ϕ^*
(2.172, 4.247)	0, π
(4.247, 4.257)	0, $0 < \phi^* < \pi$, π, -ϕ^*
(4.257, 4.381)	0, $0 < \phi^* < \pi$, -ϕ^*
(4.381, 6.223)	$0 < \phi^* < \pi$, -ϕ^*
(6.223, 6.407)	0, $0 < \phi^* < \pi$, -ϕ^*
(6.407, 8.468)	0, π

The fact that there are ten bifurcations across the range of τ where the stable steady states change indicates that the qualitative dynamics of the weakly-connected system, and therefore its ability to synchronize, is remarkably sensitive to the value of the time delay τ. Increasing τ from 0 to T can produce a full range (i.e., from 0 to 2π) of stable phase differences ϕ^* (Table 1). This enriches our understanding and ability to predict the dynamics of the system beyond the $\tau = 0$ case with only two stable steady states (0 and π). When $\tau > 0$ it is still possible to have 0 and/or π as a stable steady state, but other asynchronous stable steady states are available as well over some values of τ. However, there are also ranges of τ values where the steady states 0 and π become unstable, separated by stable asynchronous steady states. Overall, our bifurcation diagram (Figure 3) can be used to show that the fraction of τ values (of the full range length T) where in-phase synchronization is possible (i.e., 0 is a stable steady-state) is $(0.0228 + (4.381 - 2.172) + (8.468 - 6.223))/T = 0.529$. This means that approximately half of all possible time delays (on the same order of magnitude as T or less) prevent in-phase synchronization given the parameter values we used in numerical simulations.

In fact, the system loses its ability to synchronize in-phase (i.e., the steady state 0 becomes unstable) even with a very small time delay. If τ were increased from 0 to just 0.0228 (a time delay of $0.0228/\alpha$ in unscaled time), a population with in-phase synchronized dynamics would bifurcate to a non-zero stable steady state, decreasing the risk of simultaneous extinction in both patches. The phase difference would remain held away from in-phase synchronization as τ is increased, all the way until $\tau = 2.172$. This sensitivity of the dynamics to small changes of τ also means that if two patches are synchronized in-phase, their global (simultaneous) risk of extinction can be reduced by a change in the delay τ of less than $(8.468 - 6.223)/2 = 1.123$ to bring the dynamics to a sub-critical pitchfork bifurcation where the system shifts to another non-zero steady state, or to a super-critical pitchfork bifurcation where the steady-state phase difference smoothly increases from zero.

6.2 Rate of convergence to synchrony

Previous studies by Goldwyn and Hastings (2008) have shown that in general, relaxation oscillators converge to steady-state dynamics faster than other types of oscillators (due to their iPRCs having greater maximum magnitudes). We find that within this category of relaxation oscillators, a time delay plays a significant role in further determining how strong a synchronizing force weak dispersal can be. We find that convergence strength to synchrony predicted by the model varies widely over the range of τ values we consider, and in a way that indicates that the system is highly sensitive to small changes of τ.

The convergence rate to synchrony of a stable steady-state ϕ^* is calculated as $|G'(\phi^*)|$, the absolute value of the first derivative with respect to ϕ of the function $G(\phi)$, evaluated at ϕ^*; or in other words, the absolute value of the slope of the graph of $G(\phi)$ at the zero ϕ^* (the slope will be negative if ϕ^* is a stable steady-state). The greater the convergence rate to synchrony, the shorter the time for transient dynamics around the steady-state; and the more likely it is to be observed in natural systems exposed to recurring perturbations away from their phase-locked state.

Our analysis shows that weak, non-delayed dispersal is not in itself a strong mechanism of in-phase synchrony in terms of convergence strength, compared to delayed dispersal. This is revealed by the slow convergence to in-phase synchrony at $\tau = 0$ compared to those systems with delayed dispersal ($\tau > 0$)

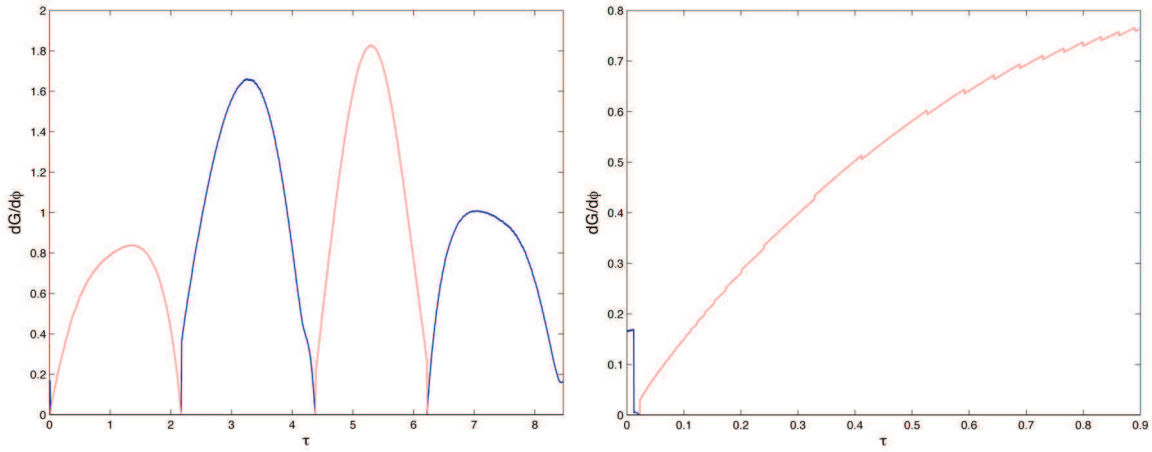

(a) (b)

Fig. 4 $\varepsilon = 0.1$, $\alpha = 0.3$, $\mu = 0.3$, and $\delta = 0.001$. Rate of convergence to stable steady-state 0 (blue) or the next stable steady state $\phi^* > 0$ (red) if 0 is unstable. (a) shows the values for the full τ range, (b) shows a zoom of (a) for values closer to $\tau = 0$.

that have an in-phase stable equilibrium (*e.g.* $\tau = 3.2$ or $\tau = 6.9$; Figure 4). More specifically, the rate of convergence to a stable $\phi^* = 0$, or to the steady state with the smallest phase difference, is faster with than without a time delay (Figure 4). This is because at $\tau = 0$ the system is close to the pitchfork bifurcation observed at $\tau = 0.0228$ where 0 loses its stability, and it is precisely at that bifurcation points that $G'(\phi) = 0$ and that the convergence rate is minimum. Convergence rate is fastest at the centres of the intervals between consecutive bifurcations points: these are the τ values where weak dispersal is able to best produce synchronized dynamics in nature. Because there is a bifurcation very close to $\tau = 0$, a slight increase in τ from zero not only creates asynchronous phase-locking possibilities, but also increases the rate of convergence to these phase-locked states, and thus the predicted ability of weak dispersal to explain synchrony in nature. Thus, we have shown that for a specific set of parameters corresponding to oscillatory dynamics of a single predator-prey patch, even a very small time delay can produce dynamics that are markedly different from the predictions of the non-delayed model. We conducted a sensitivity analysis showing the robustness of this result to a broad range of predator and prey parameter values (ε, α, and μ; see Appendix B.

7 Discussion

The importance of a landscape matrix in controlling movement of individuals and propagules between discrete populations has led to its integration into recent management and conservation practices, but most theoretical frameworks of patch dynamics are still based on instantaneous dispersal. Our time-delay approach to modeling dispersal in a patch model constitutes a simple way to incorporate details of individual movement through the landscape matrix within a patch dynamics framework. We show that our patch model with delayed dispersal provides a useful approximation of dispersal through continuous landscapes. Our results show that dispersal time is a spatial process deserving of attention when considering synchronization dynamics. We more precisely show how delayed dispersal can greatly limit the ability of weak dispersal to synchronize predator-prey dynamics to in-phase dynamics, which put a system at highest risk of global extinction. Instead, delayed dispersal is predicted to promote asynchronous phase-locked dynamics across discrete populations. Our results have important implications for understanding causes of spatial synchrony in natural systems and for bridging gaps between simple patch models and landscape ecology.

7.1 Knowing when to be discrete, and when to be continuous

Patch dynamics with delayed dispersal can provide a very useful tool to approximate complex movement patterns across natural landscape matrices. This approach effectively embeds a patch model onto a

more concrete physical space resembling a fragmented landscape, where local patches are separated by significant space that individuals disperse across. The modeling technique for dispersal here is applicable to any such system in nature where patches are not directly next to each other (in which case τ would just be zero), even if there's only a small transmission time between patches: there is no limit in general to how sensitive a system can be to small transmission delays.

The notion of time delays in dispersal can be extended to systems involving egg banks, seed banks, dia-pausing eggs, or dormant stage in general. It is usually thought that a dormant stage is a means of "dispersal through time" to increase survival through harsh conditions (Callaghan and Karlson 2002). However, many examples of dormant stages also involve spatial aggregation and thus movement between dormant and non-dormant stages (Rothhaupt 2000). Such situations where dormant propagules disperse through space are just an extreme example of the complex ways that dispersal through space and time are coupled and can explain important ecological phenomena such as persistence and coexistence through storage effects (Chesson 2000). Our work shows indeed that spatial aggregation comes hand in hand with temporal segregation, which provides a relevant and insightful approach to modeling population dynamics in spatial systems.

7.2 Time-delayed dispersal and synchrony

Identifying causes of synchrony remains a major challenge in many biological systems. Ecologists have provided both theoretical and empirical evidence for weak dispersal as an important cause of spatial synchrony between discrete populations (see Liebhold 2004 for a review), but the question remains: when can weak dispersal be the mechanism behind in-phase synchronization between natural populations that are typically exposed to frequent phase perturbations and embedded within complex landscapes? Goldwyn and Hastings (2008) showed that a requirement for weak dispersal to cause synchronization in a network of predator-prey patches in nature is that the predator-prey dynamics behave as a relaxation oscillator. Relaxation oscillations result from a separation of temporal scales between predator and prey dynamics and lead to fast convergence time to in-phase steady state synchrony. Within this region of parameter space, our study provides a new perspective on the ability of weak dispersal to cause synchronization across natural landscapes where dispersal between habitats is delayed.

Our time-delayed dispersal approach gives a way of using information we may have about a system connected through weak dispersal (the distance between patches, speed of the dispersers, etc.) to infer the importance of weak dispersal as an important factor behind synchronized dynamics. Our results show that the delay itself can have a number of implications for phase dynamics: systems may be carried away from in-phase synchronization and held at a non-zero phase-locking state. Over a range of delay values (τ) the system may increase from two to four the number of stable phase-locked steady states, further reducing the parameter space resulting in in-phase synchronization. Our results also relate the value of τ to the rate of convergence to in-phase synchrony and show how a time delay can greatly impede the ability of weak dispersal to explain the maintenance of in-phase synchrony in nature, and instead enhance phase-locked dynamics. The rate of convergence is important because in nature where systems frequently experience perturbations due to stochastic fluctuations in the environment, their steady state dynamics are unlikely to be observed unless they recover quickly relative to the frequency of perturbations. In agreement with more general bifurcation theories (Strogatz 2000), our results show that the convergence rate is minimum near τ bifurcation thresholds, and is maximum between these bifurcation points. This is especially relevant because for a broad range of ε–α–μ values, in-phase synchrony bifurcates to phase locking at delay values very close to $\tau = 0$. Instantaneous dispersal dynamics is thus highly sensitive to the introduction of arbitrarily small dispersal time.

Our results suggest that the combined knowledge of all stable phase-locked states and of their convergence strength is important to predict when weak dispersal can be a very important cause of synchronization for systems characterized by relaxation oscillations. An example of such a system are those involving insect outbreaks, which commonly produce large amplitude oscillations (Peltonen et al. 2002). In communities characterized by small amplitude and sinusoidal oscillations, such as in the hare-lynx system, weak dispersal is an unlikely cause of synchronization, and extra information about the transmission delay may not be useful. Such systems are more likely to be synchronized through the Moran effect (Goldwyn and Hastings 2008), or by strong dispersal as dispersal strength decreases convergence

time. (The convergence rate $|G'(\phi^*)|$ in our model inherits the factor δ from $G(\phi)$ – see (4.5) or (5.1) – and so the convergence rate is proportional to δ and the convergence time is proportional to $1/\delta$.)

7.3 Patch dynamics within landscape matrices

Fragmented landscapes are typically formed of habitats, connecting corridors, and the overall landscape matrix (Turner et al. 2001). Dispersal time captures a number of landscape properties: spatial arrangement of habitats, the presence and effectiveness of corridors, and the resistance of the landscape matrix to movement (Koh et al 2010). The idea of movement time (time-delay) between habitat fragments as assumed in our study can inform on the role of habitat corridors in connecting wildlife refuges. The use of these corridors in fragmented habitats to assist the dispersal of endangered species and decrease the risk of regional extinction is still controversial (Brady et al. 2011), and could be resolved through the understanding of dispersal delays across landscapes.

While the presence of a landscape matrix and of corridors involve a finite dispersal time between habitats, it can also affect demographic processes and behavior of dispersing individuals, as well as regulate the rate of dispersal and modulate the coupling strength between habitats (Koh et al 2010). The phase-model we adopted allows studying movement time within a patch dynamical framework, but it also assumes weak dispersal and no change in individual density or behavior during dispersal. Future work should investigate the importance of a transmission delay with stronger dispersal coupling using delay-differential equations. The integration of demographic processes such as mortality during dispersal would also improve the relevance of patch dynamical models for understanding synchrony across complex landscapes. We hope our modeling approach can integrate these more realistic assumptions that are key to conservation, while still contributing to a more general theory of patch dynamics.

Acknowledgements E. Wall is grateful to the McGill University Biology Department for a Science Undergraduate Research Award (SURA). F. Guichard and A.R. Humphries thank the Natural Sciences and Engineering Research Council of Canada (NSERC) for funding though the Discovery Grants Program.

References

1. Allen LJS (1983) Persistence and Extinction in Lotka-Volterra Reaction-Diffusion Equations. Math Biosci, 65(1):1-12. doi: 10.1016/0025-5564(83)90068-8
2. Blasius B, Tönjes R (2007) Predator-prey oscillations, synchronization and pattern formation in ecological systems. In: L. Schimansky-Geier, B. Fiedler, J. Kurths, E. Schöll (eds) Analysis and Control of Complex Nonlinear Processes in Physics, Chemistry and Biology. World Scientific, Singapore, pp 397-427
3. Brady MJ, McAlpine CA, Possingham HP, Miller CJ, and Baxter GS (2010) Matrix is important for mammals in landscapes with small amounts of native forest habitat. Landscape Ecology, 26(5):617-628
4. Byers JA (2001) Correlated random walk equations of animal dispersal resolved by simulation. Ecol, 82(6):1680-1690. doi: 10.2307/2679810
5. Callaghan T and Karlson R (2002) Summer dormancy as a refuge from mortality in the freshwater bryozoan plumatella emarginata. Oecologia, 132(1):51-59
6. Campbell SA and Kobelevskiy I (2012) Phase models and oscillators with time delayed coupling. Discrete and Continuous Dynamical Systems, 32(8):2653-2673
7. Chesson P (2000) Mechanisms of maintenance of species diversity. Annual Review of Ecology and Systematics, 31:343
8. Dhamala M, Jirsa V, and Ding M (2004) Enhancement of neural synchrony by time delay. Physical Review Letters, 92(7):074104
9. Durrett R, Levin S (1994) The importance of being discrete (and spatial). Theo Popul Biol, 46:363-394. doi: 10.1006/tpbi.1994.1032
10. Ermentrout GB (1994) In: Ventriglia F (ed) Neural Modeling and Neural Networks. Pergamon Press, Oxford
11. Ermentrout GB (2002) Simulating, Analyzing, and Animating Dynamical Systems. SIAM
12. Goldwyn EE, Hastings A (2008) When can dispersal synchronize populations?. Theo Popul Biol, 73:395-402. doi: 10.1016/j.tpb.2007.11.012
13. Hanski I (1999) Metapopulation ecology. Oxford University Press, Oxford.
14. Hoppensteadt FC, Izhikevich EM (1997) Weakly Connected Neural Networks. Springer-Verlag, New York
15. Izhikivech EM (2008) Phase models with explicit time delays. Phys Rev E, 58:905-908. doi: 10.1103/PhysRevE.58.905
16. Kobelevskiy I (2008) Bifurcation analysis of a system of Morris-Lecar neurons with time delayed gap junctional coupling. Masters Dissertation, University of Waterloo, Canada.
17. Koh LP, Lee TM, Sodhi NS, and Ghazoul J (2010) An overhaul of the species-area approach for predicting biodiversity loss: incorporating matrix and edge effects. Journal of Applied Ecology, 47(5):1063-1070
18. Kuramoto Y (1984) Chemical Oscillations, Waves, and Turbulence. Springer-Verlag, Berlin
19. Levins R (1969) Some demographic and genetic consequences of environmental heterogeneity for biological control. Bulletin of the Entomological Society of America, 15:237-240.

20. Liebhold A, Koenig W, Bjørnstad O (2004) Spatial synchrony in population dynamics. Annu Rev Ecol Evol Syst, 35:467-490. doi: 10.1146/annurev.ecolsys.34.011802.132516
21. Moran PAP (1953) The statistical analysis of the Canadian lynx cycle. II. Synchronization and metereology. Aust J Zool, 1:291-298.
22. Othmer HG, Dunbar SR, Alt W (1988) Models of dispersal in biological systems. Journal of Math Ecol, 26(3):263-98. doi: 10.1007/BF00277392
23. Peltonen M, Liebhold A, Bjornstad O, and Williams D (2002) Spatial synchrony in forest insect outbreaks: Roles of regional stochasticity and dispersal. Ecology, 83(11):3120-3129
24. Ranta E, Kaitala V, Lundberg P, 1998. Population variability in space and time: the dynamics of synchronous populations. Oikos, 83:376-382. doi: 10.2307/3546852
25. Rothhaupt K (2000) Plankton population dynamics: food web interactions and abiotic constraints. Freshwater Biology, 45(2):105-109
26. Schuster, H and Wagner P (1989) Mutual entrainment of 2 limit-cycle oscillators with time delayed coupling. Progress of Theoretical Physics, 81(5):939-945
27. Strogatz SH (2000) Nonlinear dynamics and chaos with applications to physics, biology, chemistry, and engineering. Westview Press, Cambridge, Mass
28. Turchin P (1998) Quantitative analysis of movement : measuring and modeling population redistribution in animals and plants. Sinauer Associates, Sunderland, Mass
29. Turner MG, Gardner RH, and O'Neill RV (2001) Landscape ecology in theory and practice: pattern and process. Springer, New York
30. Winfree AT (1980) The Geometry of Biological Time. Springer, New York

Appendix A

For ease of analysis in studying synchronization with the assumption of weak dispersal, we reduce the full two-patch model (3.3) to a phase model using concepts from weakly connected network theory (see (Hoppensteadt and Izhikevich 1977)). Here we expand on the phase model reduction used in Section 4, to understand how the general principles of weakly connected network theory can be used on a general system viewed from a coupled oscillator perspective. A weakly connected network in general is any system of the form

$$\frac{dX_i}{dt} = F_i(X_i) + \delta W_i(X_1, \ldots, X_n), \quad i = 1, \ldots, n, \tag{A.1}$$

where each $X_i(t) \in \mathbb{R}^m$ and δ is a small parameter. (For now we do not consider a time delay in coupling.) We are interested in the case where each decoupled subsystem ($\delta = 0$)

$$\frac{dX_i}{dt} = F_i(X_i), \quad i = 1, \ldots, n \tag{A.2}$$

has an exponentially orbitally stable limit cycle attractor $\gamma_i \subset \mathbb{R}^m$.

The limit cycle γ_i being a periodic orbit of the system, has an associated period T_i and a natural frequency $\Omega_i = 2\pi/T_i$. As a closed curve through m-dimensional space, each γ_i can be parameterized with a phase variable θ_i that increases by 2π in one period. With an arbitrary starting point $p_i \in \gamma_i$, we define a mapping $P_i : [0, 2\pi) \to \mathbb{R}^m$ that takes $\theta_i \in [0, 2\pi)$ to the unique corresponding point on γ_i that is $P_i(\theta_i) = Y_i(\theta_i/\Omega_i) = Y_i(\theta_i T_i/2\pi)$, where $Y_i(t) \in \mathbb{R}^m$ solves $dY_i(t)/dt = F_i(Y_i(t))$ with $Y_i(0) = p$ ($Y_i(t)$ is on the limit cycle γ_i) (Hoppenseadt and Izhikevich 1977).

The fact that the γ_i are exponentially orbitally stable limit cycle attractors means that for small δ, coupling between the X_i only significantly affects the phase variables θ_i. For systems where oscillators have identical frequencies $\Omega_1 = \cdots = \Omega_n = \Omega$, Malkin's Theorem says that solutions of the system (A.1) can be continuously mapped to solutions of the following canonical phase model defined on the n-torus $\mathbb{T}^n = \mathbb{S}^1 \times \cdots \times \mathbb{S}^1$ (Hoppensteadt and Izhikevich 1977):

$$\frac{d\theta_i}{dt} = \Omega + \delta H_i(\theta_1 - \theta_i, \ldots, \theta_n - \theta_i) + \mathcal{O}(\delta^2), \quad i = 1, \ldots, n, \tag{A.3}$$

where H_i are phase coupling functions,

$$H_i(\theta_1 - \theta_i, \ldots, \theta_n - \theta_i) = \frac{1}{T}\int_0^T \hat{\gamma}_i(t) \cdot W_i(\gamma_1(t + (\theta_1 - \theta_i)/\Omega), \ldots, \gamma_n(t + (\theta_n - \theta_i)/\Omega))dt \tag{A.4}$$

and $\hat{\gamma}_i(t)$ solves the system

$$\begin{aligned} \frac{dz(t)}{dt} &= -DF(\gamma_i(t))^T z(t) \\ z(t) \cdot \gamma_i{}'(t) &= 1. \end{aligned}$$

The function $\hat{\gamma}_i(t)$ is referred to as the infinitesimal phase response curve (iPRC) (Winfree 1980; Kuramoto 1984), measures the degree to which an arbitrarily short and infinitesimally small perturbation advances (positive valued) or slows (negative valued) the phase (Goldwyn and Hastings 2008). The iPRC can be thought of as a measure of the sensitivity of the oscillator to perturbations at each time t in $[0, T_i)$: at times when the oscillator is affected most by perturbations (from dispersal), the iPRC has a greater maximum magnitude. Goldwyn and Hastings (2008) show that the greater the separation in predator-prey timescales (*i.e.*, relaxation oscillator), the greater the sensitivity of the oscillator to perturbations, and the higher the maximum magnitude of the prey component in the iPRC (Table 2). This explains why relaxation oscillators converge faster to synchrony than more sinusoidal oscillators. It also underlies the requirement for separated timescales between predator and prey for weak coupling to result in synchronization in natural systems (Goldwyn and Hastings 2008).

Crucially, phase model reduction is also possible for weakly connected systems involving an explicit dispersal delay. The phase model for such systems is derived in (Hoppensteadt and Izhikevich 1977) and (Ermentrout 1994). For weak coupling and $\mathcal{O}(1)$ delays (i.e., delays of the same order of magnitude as the period of oscillation or less), the delays do not explicitly appear in the phase model, but rather result in an additional phase shift. The main theorem of weakly connected delayed systems is stated as follows, adapted from (Hoppensteadt and Izhikevich 1977) and (Izhikevich 2008):

Theorem (Phase model with delayed coupling): *Consider a weakly connected oscillatory network that has an explicit transmission delay, described by the system*

$$\frac{dX}{dt}_i = F_i(X_i) + \delta W_i(X_1(t-\eta_{i1}), \ldots, X_n(t-\eta_{in}); \;\; X_i \in \mathbb{R}^m, \quad i = 1, \ldots, n, \tag{A.5}$$

where the η_{ij} are finite nonnegative real numbers, all $\mathcal{O}(1)$. Suppose that each uncoupled system has an exponentially orbitally stable T-periodic limit cycle solution $\gamma_i \subset \mathbb{R}^m$. Then, the system can be reduced to the phase model

$$\frac{d\theta_i}{dt} = \Omega + \delta H_i(\theta_1 - \theta_i - \Phi_{1i}, \ldots, \theta_n - \theta_i - \Phi_{1i}) + \mathcal{O}(\delta^2), \quad i = 1, \ldots, n, \tag{A.6}$$

where $\Phi_{ji} = \Omega\eta_{ji} \mod 2\pi$, and the H_i functions are defined by (A.4).

Appendix B

We examine specifically how varying the parameters ε, α and μ might affect the general results we showed for a specific set of parameters leading to oscillatory dynamics of a single predator-prey patch. Table 2 shows the parameter sets, as well as the maximum magnitude of the iPRC at these parameter values. As expected, decreasing α and μ (we keep $\varepsilon = 0.1$) increases the height of the iPRC. Figures 5 and 6 shows the bifurcation diagrams analogous to Figure 3 for a number of other parameter sets. Similarly to the parameter set used for our main analysis, varying τ across the interval $[0, T]$ changes the dynamics and rates of convergence to steady states as the dynamics bifurcate a number of times. The bifurcation diagrams close to $\tau = 0$ in Figure 6 show that there is a range of parameter space where $\phi^* = 0$ is stable at $\tau = 0$, but very close to a bifurcation, so that with even a slight increase in τ, the system can move to asynchrony with a much faster convergence rate. Investigating this slightly larger region of ε–α–μ phase space indicates that our qualitative results for the first set of parameters are generally comparable to other parameter sets, and that decreasing α and μ (separating the predator-prey timescales and making the oscillator relaxation-like) mainly has an effect that shows up on the dynamics at $\tau = 0$.

Table 2 Parameter sets.

Parameter set	ε	α	μ	iPRC (adjoint) height
1	0.1	0.2	0.15	2.25×10^{20}
2	0.1	0.2	0.3	1.3×10^{8}
3	0.1	0.2	0.35	2.5×10^{6}
4	0.1	0.2	0.45	1.1×10^{4}
5	0.1	0.25	0.2	3.6×10^{10}
6	0.1	0.25	0.3	1.0×10^{5}
7	0.1	0.25	0.4	900
8	0.1	0.25	0.5	46
9	0.1	0.3	0.1	7.0×10^{14}
10	0.1	0.3	0.15	1.0×10^{9}
11	0.1	0.3	0.3	1600
12	0.1	0.3	0.35	300
13	0.1	0.3	0.45	20
14	0.1	0.35	0.1	4.5×10^{10}
15	0.1	0.35	0.2	1.8×10^{4}
16	0.1	0.35	0.3	140
17	0.1	0.35	0.4	12
18	0.1	0.4	0.05	2.5×10^{17}
19	0.1	0.4	0.15	4.5×10^{5}
20	0.1	0.4	0.25	130
21	0.1	0.4	0.35	11
22	0.1	0.45	0.1	1.0×10^{6}
23	0.1	0.45	0.2	180
24	0.1	0.45	0.3	12

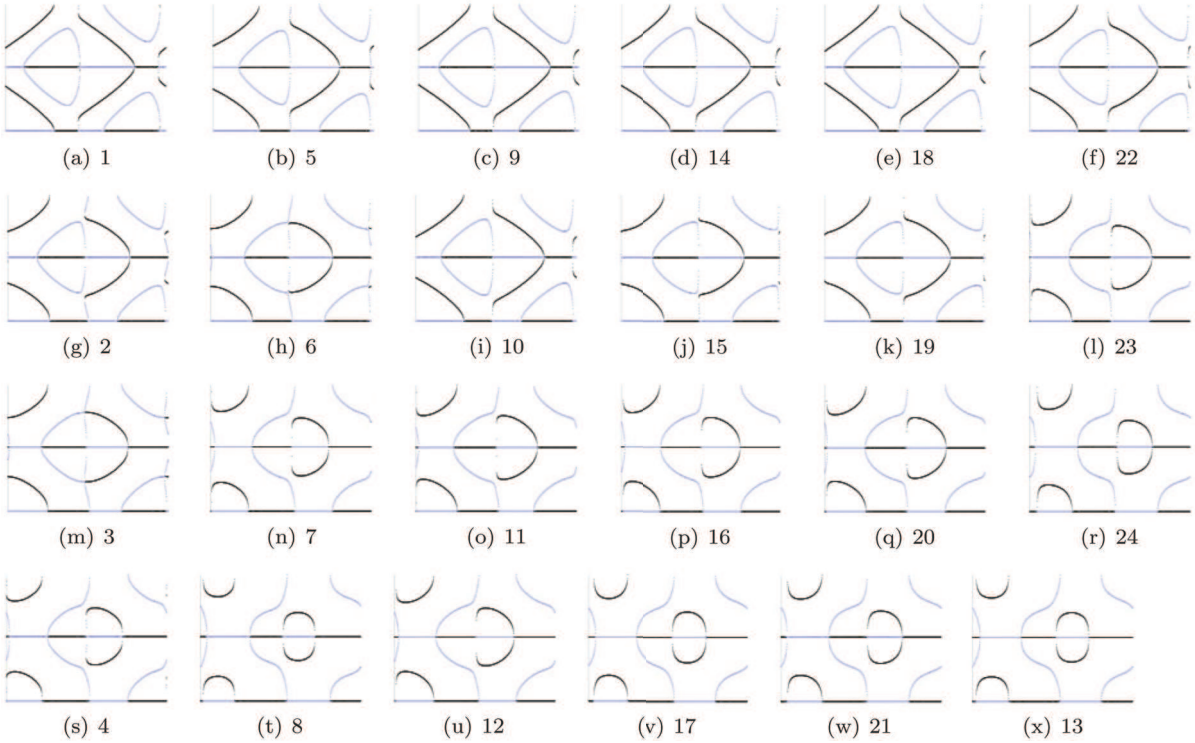

Fig. 5 $\delta = 0.001$; refer to Table 2 for parameter set values corresponding to numbers 1 through 24. τ Bifurcation diagrams (full range of τ from 0 to T) through a region of ε–α–μ parameter space. Stable steady-states are black; unstable steady-states are blue.

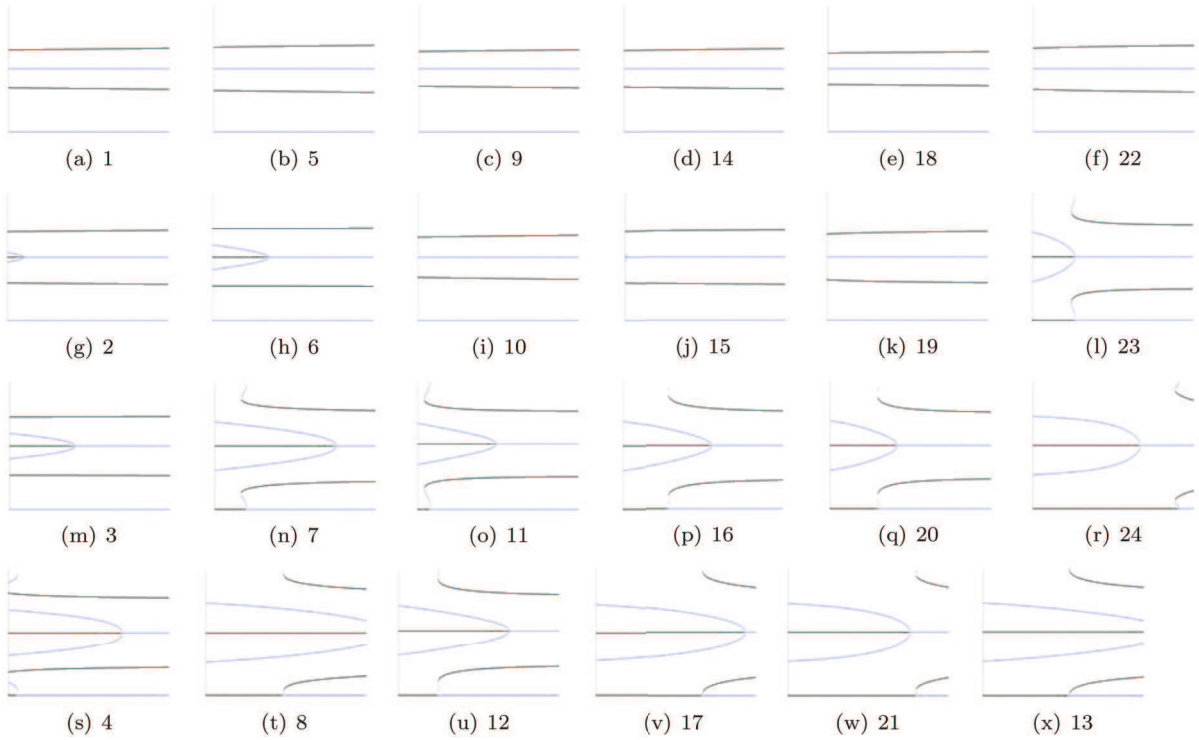

Fig. 6 $\delta = 0.001$; refer to Table 2 for parameter set values corresponding to numbers 1 through 24. τ Bifurcation diagrams (τ from 0 to 0.3) through a region of ε–α–μ parameter space. Stable steady-states are black; unstable steady-states are blue.